The critical role of the boreal summer mean state in the development of the IOD

Baoqiang Xiang,[1,2] Weidong Yu,[2] Tim Li,[1,3] and Bin Wang[1,3]

Received 13 October 2010; revised 23 November 2010; accepted 27 December 2010; published 29 January 2011.

[1] Boreal summer is a critical season for the rapid development of the Indian Ocean Dipole (IOD). In this study, three factors related to the boreal summer mean state are proposed to be important for the rapid development of the IOD, by strengthening the equatorial zonal wind anomaly and thus the dynamic Bjerknes feedback. Firstly, as part of the Indo-Pacific warm pool, the high mean SST in the southeastern tropical Indian Ocean (SEIO) acts as an essential prerequisite for the development of anomalous convection. Secondly, the maximum of the suppressed precipitation in response to a cold SST anomaly (SSTA) in the SEIO, shifts northward towards the equator because the mean precipitation is equatorially trapped in boreal summer. Thirdly, the monsoonal easterly shear in boreal summer promotes an enhanced, more equatorially symmetric low-level Rossby wave response to a prescribed equatorially asymmetric heating over the SEIO. The above three processes promote a greater equatorial zonal wind response and thus a greater Bjerknes feedback, as well as a greater IOD development during boreal summer. **Citation:** Xiang, B., W. Yu, T. Li, and B. Wang (2011), The critical role of the boreal summer mean state in the development of the IOD, *Geophys. Res. Lett.*, *38*, L02710, doi:10.1029/2010GL045851.

1. Introduction

[2] As one of the dominant interannual modes in the tropical Indian Ocean, the Indian Ocean Dipole (IOD) involves active ocean-atmosphere interactions [*Saji et al.*, 1999; *Webster et al.*, 1999; *Li et al.*, 2003]. One salient characteristic of the IOD is its phase-locking to the annual cycle, that is, the IOD grows rapidly in boreal summer and reaches a peak phase in boreal fall [*Saji et al.*, 1999; *Li et al.*, 2003; *Hong et al.*, 2008a, 2008b; *Halkides and Lee*, 2009]. During boreal summer, the atmosphere-ocean interactions invoking two important positive feedback processes were proposed to have critical effects on the rapid development of the IOD. One is the equatorial Bjerknes [*Bjerknes*, 1969] feedback between the equatorial surface zonal wind and the SST anomaly (SSTA) through the thermocline displacement and upwelling [*Saji et al.*, 1999; *Li et al.*, 2003; *Hong et al.*, 2008a, 2008b; *Halkides and Lee*, 2009], and the other is the wind-evaporation-SST feedback [*Wang et al.*, 2003; *Li et al.*, 2003; *Halkides et al.*, 2006]. The southeasterly monsoonal flow in northern summer over the southeastern tropical Indian Ocean (SEIO) is crucial in promoting a season-dependent coupled atmosphere-ocean instability, allowing a wind-evaporation-SST feedback to become efficient between an atmospheric Rossby wave-induced anticyclonic anomaly and a cold SSTA off Sumatra/Java during boreal summer [*Wang et al.*, 2003; *Li et al.*, 2003; *Halkides et al.*, 2006]. The southeasterly flow also offers a 'seasonal-window' for the development of the Bjerknes feedback, because during that season the mean thermocline is shallow and the ocean upwelling is strong near the Sumatra/Java coast [*Xie et al.*, 2002].

[3] The observed equatorial easterly wind anomaly, acting as an integral component of the Bjerknes feedback, is essential for the IOD development. Similar to the ENSO diagnosis [*Guilyardi et al.*, 2009], one may define the air-sea coupling strength as the ratio of the equatorial zonal wind anomaly (averaged over the blue box in Figure 1b) to the SSTA in the SEIO (averaged over the red box in Figure 1a) based on their spatial patterns. This ratio represents the response of the equatorial zonal wind anomaly to per-unit change of the SSTA. Our calculation shows that the coupling strength is 3.2 m/s/K in the equatorial Indian Ocean, which is more than 2 times greater than 1.5 m/s/K in the equatorial Pacific. The latter is estimated by the ratio of the zonal wind anomaly in the Niño-4 region to the SSTA in the Niño-3 region [*Guilyardi et al.*, 2009], from the composite of three extreme Niño events (1982, 1986, 1997). The result above implies that the equatorial atmospheric response to the SSTA is stronger in the tropical Indian Ocean than in the tropical Pacific. Understanding the cause of this holds a key for understanding the rapid development of the IOD during boreal summer.

2. Data and Methodology

[4] Primary data used in this study are monthly mean SST from ERSST (NOAA Extended Reconstructed SST) [*Smith and Reynolds*, 2003], monthly mean precipitation from Global Precipitation Climatology Project (GPCP) datasets [*Adler et al.*, 2003], and monthly mean surface (1000 hPa) wind from NCEP-DOE (National Centers for Environmental Prediction–Department of Energy) Reanalysis 2 products [*Kanamitsu et al.*, 2002]. In this study, the period between 1979 and 2009 is chosen because of the availability of data, and a linear trend has been removed for all these data. Similar to *Hong and Li* [2010], a positive IOD case is defined with the averaged SSTA over the domain (0–10°S, 90°–110°E) less than 0.4 standard deviation during the IOD mature phase (September–November). Therefore, six cases (1982, 1983, 1994, 1997, 2003, 2006) are selected for the

[1]Department of Meteorology, School of Ocean and Earth Science and Technology, University of Hawaii at Manoa, Honolulu, Hawaii, USA.
[2]Research Center of Ocean Climate, First Institute of Oceanography, SOA, Qingdao, China.
[3]International Pacific Research Center, Honolulu, Hawaii, USA.

0094-8276/11/2010GL045851

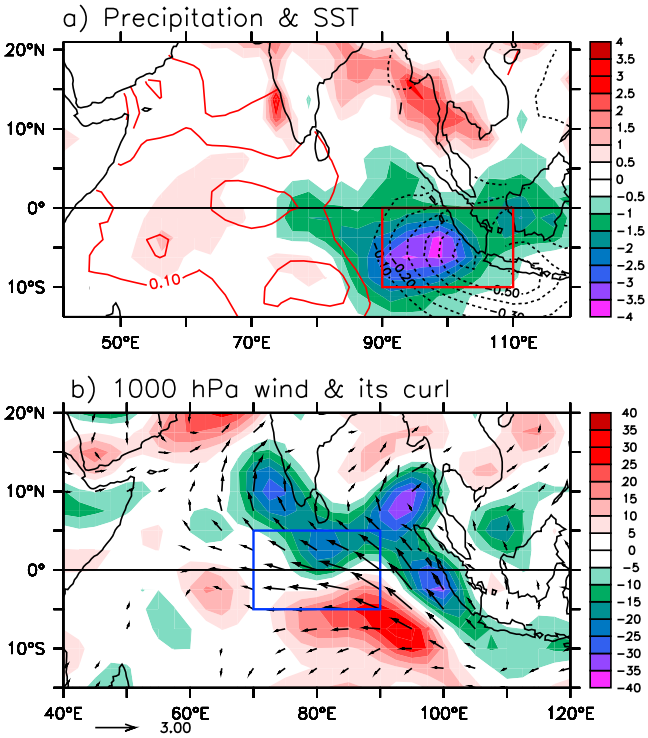

Figure 1. (a) Composite precipitation anomaly (shading, mm/day) and SSTA (contours, °C). (b) Composite 1000 hPa wind anomaly (vectors, not shown when the wind speed is less than 0.3 m/s) and the corresponding wind curl (shading, 10^{-7} s^{-1}) during July–August for the positive IOD events. Composite is computed based on six recent IOD events, 1982, 1983, 1994, 1997, 2003, 2006.

composite analysis in this study. Several cases (such those in 1985, 1986, 1999) are not included as they do not exhibit typical IOD patterns.

[5] Two atmospheric AGCMs, the ECHAM4 and a dry AGCM, are used in this study. The ECHAM4 model is developed from Max-Planck-Institute (MPI) for Meteorology in Hamburg [*Roeckner et al.*, 1996]. We use a version with T42 resolution in the horizontal and 19 levels in the vertical. Three sets of experiments are carried out. The control run is a 20-yr run forced by the observed climatological SST and sea ice. Two sensitivity experiments are further conducted by imposing the observed composite cold SSTA in the SEIO (i.e., black contours in Figure 1a) during July–August (JA) and during January–February (JF), with 20 ensemble members each. For each ensemble run, the initial condition is perturbed by adding day-to-day root-mean-square differences of zonal wind, meridional wind, temperature and specific humidity fields. For all sensitivity experiments, the model is integrated for two months.

[6] A dry AGCM is also used which is built based on a dry version of Princeton AGCM with five sigma levels. It is linearized by a prescribed 3D basic flow, derived based on the long-term NCEP-NCAR (National Center for Atmospheric Research) reanalysis data [*Kalnay et al.*, 1996]. Details about this model were described by *Jiang and Li* [2005] and *Li* [2006]. Three dry AGCM experiments are conducted. The first is a control run with a resting environment (i.e., zero mean flow). The other two are sensitivity experiments with a specified boreal summer and boreal winter mean flow. For all these experiments, the anomalous heating is estimated based on the observed composite of precipitation anomaly (Figure 1a), with a maximum amplitude about –1.6 K/day at the level of sigma = 0.3 (about 300 hPa). The model is integrated for 20 days to get a steady state response.

3. Results

[7] One direct explanation for the stronger air-sea coupling strength in the tropical Indian Ocean, is attributed to a higher mean SST in the tropical Indian Ocean than the tropical Pacific. A same magnitude of SST perturbation may induce a greater precipitation and wind response in the SEIO. In other words, atmospheric convection and wind responses are more sensitive to SST fluctuations in the warm pool than in the cold tongue [*Li et al.*, 2003].

[8] In distinctly different from the ENSO in the tropical Pacific, another interesting feature of the IOD is that the cold SSTA in the SEIO shows a marked asymmetry with the greatest SST cooling occurring to the south of the equator (Figure 1a). Based on *Gill* [1980]'s theory, one would expect a pronounced meridional wind rather than zonal wind response at the equator in response to this asymmetric SSTA forcing. This would prohibit the Bjerknes feedback. The observed wind curl, however, shows a rather symmetric feature, with a pronounced zonal wind anomaly at the equator (Figure 1b, also see *Yu et al.* [2005, Figure 1]). A more symmetric wind response favors a greater zonal wind anomaly at the equator, which promotes a greater Bjerknes feedback and thus a greater IOD development.

[9] To quantitatively measure the extent to which a variable is asymmetric about the equator, we introduce a relative symmetry index (RSI). The RSI is estimated based on the ratio of the symmetric and anti-symmetric components. A greater (smaller) RSI value indicates that the anomaly field is more symmetric (asymmetric) relative to the equator. The amplitudes of the symmetric and antisymmetric components are calculated based on averaged values in northern and southern domains, following *Li* [1997]. For the SSTA field, the northern and southern domains are (0–10°N, 90°–110°E) and (0–10°S, 90°–110°E). For the anomalous precipitation field, the northern and southern domains are (0–15°N, 85°–100°E) and (0–15°S, 85°–100°E). For the anomalous wind curl field, the northern and southern domains are (0–15°N, 80°–95°E) and (0–15°S, 80°–95°E).

[10] Our calculations show that the RSI for the SSTA (1.5) and precipitation anomaly (0.9) is one order smaller than the wind curl anomaly (23.5), indicating that the wind response is to a large extent symmetric about the equator. Why does an asymmetric SSTA forcing lead to a more symmetric surface wind response? We hypothesize that it is attributed to the effect of the boreal summer mean state. In the following, we intend to reveal the mean state effect with the aid of two types of atmospheric models.

3.1. Seasonal Dependence of Atmospheric Response to an Asymmetric SSTA Forcing

[11] To explore whether the atmospheric response to the SSTA forcing is seasonally dependent, we first examine the atmospheric response to a prescribed cold SSTA (black contours in Figure 1a) during JA and JF by using the ECHAM4 model (Figure 2). During JA (Figure 2a), the

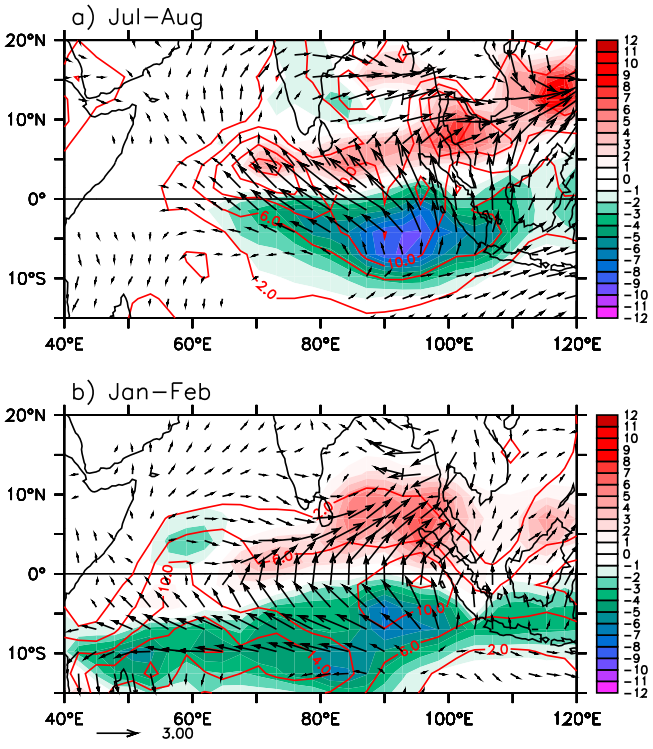

Figure 2. ECHAM4 precipitation (shading, mm/day) and 1000-hPa wind (vectors, not shown when the wind speed is less than 0.3 m/s) response to a prescribed cold SSTA pattern (black contours in Figure 1a) during (a) July–August and (b) January–February. Red contours show the model simulated climatological precipitation pattern.

ECHAM4 model simulates reasonably well the observed precipitation and surface wind anomalies, with notable below-normal precipitation south of the Equator and strong easterly anomaly over the equatorial Indian Ocean. Of particular interest is that the strength of the northern branch atmospheric Rossby wave response is more intense than its southern hemisphere counterpart in boreal summer, even though the forcing is primarily confined in the southern hemisphere.

[12] During JF, the most significant below-normal precipitation is evident in the southern ITCZ region with an east-west tilt (Figure 2b), but the precipitation anomaly near the Sumatra coast is relatively weaker than that in boreal summer. The RSI for the wind curl anomaly shows a much weaker intensity (2.0) compared to the value in boreal summer simulation (34.1) (Table 1), indicating a more asymmetric atmospheric response during boreal winter. The antisymmetric wind component with marked cross-equatorial flow is also clearly seen, which is not conducive for the Bjerknes dynamic feedback.

[13] In the boreal summer simulation, a greater equatorial zonal wind response is partly attributed to the equatorward shift of the precipitation anomaly in the SEIO. Note that the suppressed precipitation center is not collocated with the cold SSTA center, rather it shifts northwestward towards the equator. Such a phase shift feature is also seen in the observation (Figure 1a). We argue that the cause of this shift is primarily attributed to the nonlinear rectification of the background mean precipitation [*Hong et al.*, 2008a; *Hong and Li*, 2010]. The cold SSTA-induced negative precipitation anomaly cannot exceed a cap that is approximately equal to the local seasonal mean precipitation maximum. Therefore, the anomalous precipitation pattern is to a large extent modulated by the seasonal mean climate. Note that the seasonal mean precipitation in the Java coast is much less than that over the Sumatra coast (as shown in red contours in Figure 2a). A greater precipitation anomaly may appear in the latter region, even though the maximum SSTA is located in the former region.

[14] The analysis above points out the important regulation of the seasonal mean precipitation in determining the Bjerknes feedback strength. The location of the mean precipitation is more equatorially trapped during boreal summer than boreal winter (see contours in Figures 2a and 2b). As a result, the SSTA-induced precipitation anomaly is more concentrated with larger amplitude near the equator in boreal summer, which leads to a greater equatorial zonal wind response (Figure 2a). On the contrary, during boreal winter, the anomalous precipitation response is weaker and confined further to the south (shading in Figure 2b). This leads to a weaker zonal wind response at the equator.

[15] The above arguments suggest that the thermodynamic effect is of particular importance in determining the intensity of equatorial zonal wind, associated with the location shift of the anomalous heating. Additionally, the dynamic effect may also affect the anomalous wind response through an asymmetric mean flow. However, the full AGCM experiments above cannot separate these two factors. In the following, we intend to demonstrate that even given the same tropospheric heating anomaly, the atmospheric wind response could be different, due to the mean flow differences between the summer and winter.

3.2. Atmospheric Response to a Prescribed Heating in a Dry AGCM

[16] Given a prescribed diabatic heating (blue contours in Figure 3a) estimated from the observed precipitation composite (Figure 1a), we aim to examine how the atmosphere responds the anomalous tropospheric heating in the presence of the observed summer and winter 3D mean flow. For comparison we also show the model simulation in the zero mean flow.

[17] Figure 3 shows the low-level wind response in the aforementioned three mean state cases. Under a resting environment, the model simulates a pair of anticyclones on both sides of the equator, with the southern one being stronger (Figure 3a) due to a greater anomalous heating south of the equator. In the JA mean state case, this pair of anticyclones shifts northward with markedly increased intensity, especially for the northern branch (Figure 3b). The simulated low-level wind pattern agrees well with the observed (Figure 1b) and the ECHAM4 simulation (Figure 2a). In particular, the simulated easterly anomaly in the equatorial

Table 1. Relative Symmetry Index for Wind Curl Anomalies From Observations, ECHAM4 and a Dry AGCM Simulation[a]

		ECHAM4		Dry AGCM		
	Observations JA	JA	JF	Zero Flow	JA	JF
RSI	23.5	34.1	2.0	7.3	46.2	8.1

[a]RSI, relative symmetry index; JA, July–August; JF, January–February.

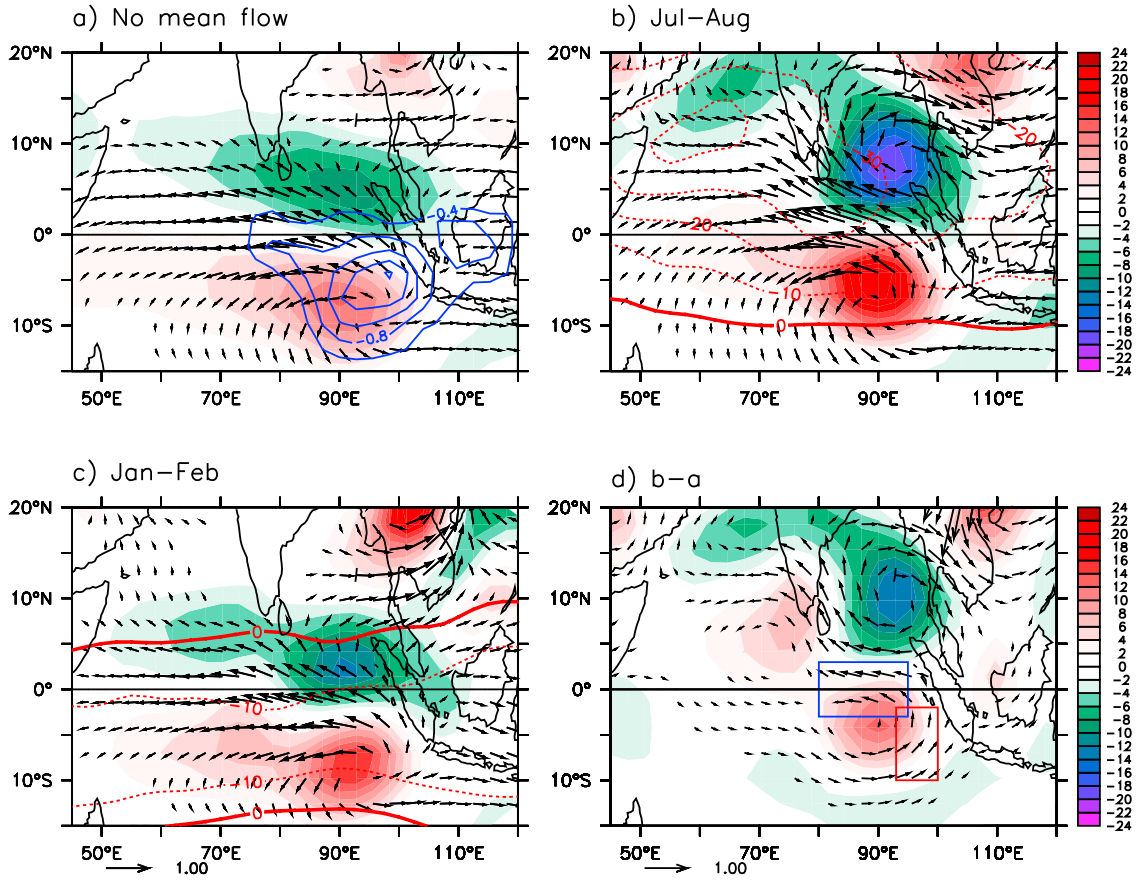

Figure 3. Dry AGCM response to a prescribed cooling forcing under (a) a zero mean flow, (b) observed July–August mean flow, (c) observed January–February mean flow, and (d) the differences between experiments in Figure 3b and Figure 3a. The vectors and shading indicate the wind anomaly (m/s; smaller than 0.1 m/s not shown) and its curl ($\times 10^{-7}$ s^{-1}) at lower level, respectively. Blue contours in Figure 3a represent the mid-tropospheric heating rate in K/day (negative). Red contours in Figures 3b and 3c are the climatological easterly vertical wind shear, with the 850 hPa zonal wind subtracted from the 200 hPa zonal wind.

Indian Ocean (blue box in Figure 3d) strengthens by about 44%, compared with the case of the zero mean flow. Such a zonal wind increase would strengthen the cold SSTA in the SEIO through the Bjerknes feedback. Meanwhile, southerly anomaly near the Sumatra coast (red box in Figure 3d) is also strengthened, which may enhance the local SSTA through anomalous vertical advection and a wind-evaporation-SST feedback [*Wang et al.*, 2003; *Li et al.*, 2003]. The simulated atmospheric low-level wind response in the JF mean flow case is in general very similar to that in the zero mean flow case. A large difference in simulated low-level wind anomalies between the full and the dry AGCMs under the winter mean state (Figures 2b and 3c) confirms that the location of anomalous convection is crucial in driving the equatorial zonal wind anomaly. The RSI calculation (Table 1) shows that the summer mean flow case attains a RSI value 5–7 times larger than those in the winter and zero mean flow cases. Therefore, we can conclude that a greater Bjerknes zonal wind-thermocline-SST feedback is likely to appear in boreal summer.

[18] Why does the summer mean flow promote a greater low-level wind response? Previous theoretical [*Wang and Xie*, 1996] and modeling [*Li*, 2006] studies suggested that the monsoonal easterly vertical shear may induce a barotropic mode response. This barotropic mode superposes the baroclinic mode, leading to a reduction (increase) of intensity of the upper level (lower level) Rossby wave response. Given that the maximum easterly shear appears north of the equator in boreal summer (see contours in Figure 3b), it is anticipated that such an equatorial asymmetry of the mean vertical shear would lead to a much enhanced low-level Rossby wave response especially for the northern branch. The difference of the equatorial zonal wind anomaly between the summer and zero mean flow cases is shown in Figure 3d. This additional barotropic mode enhances the low-level easterly anomaly west of 100°E. A much weaker modulation of the baroclinic Kelvin wave appears to the east of the heating center, consistent with the theoretical result [*Wang and Xie*, 1996]. In summary, the numerical experiments above spotlights the importance of the boreal summer mean flow in promoting a more equatorially symmetric and intense zonal wind anomaly in response to an asymmetric heating anomaly.

4. Concluding Remarks

[19] As a key component of the Bjerknes feedback, the equatorial easterly anomaly is crucial for the IOD development during boreal summer. In comparison to the ENSO in the tropical Pacific, the equatorial easterly anomaly for

the IOD exhibits a much larger magnitude in response to one-unit change of the SSTA, even though the cold SSTA is primarily confined to the SEIO.

[20] Three factors related to the boreal summer mean state are suggested to be of particular importance in determining the intensified equatorial zonal wind anomaly. Firstly, the SEIO is part of the Indo-Pacific warm pool hosting a major convection center [*Li et al.*, 2003], providing a background condition for the development of the anomalous convection. Secondly, the mean precipitation in boreal summer is more equatorially trapped than boreal winter (Figure 2), which causes a phase shift towards the equator of the anomalous precipitation center relative to the cold SSTA center. Thirdly, the stronger easterly shear in boreal summer promotes a stronger low-level Rossby wave response, leading to a more equatorially symmetric zonal wind response to a prescribed asymmetric heating. The above three factors favor a greater equatorial zonal wind anomaly, and promotes a more efficient Bjerknes feedback and a rapid IOD development. These later two mechanisms may also contribute to the rapid decay of the IOD, as the equatorial easterly wind anomaly can be substantially decreased during boreal winter even with the same cold SSTA forcing in the SEIO (Figures 2b and 3c).

[21] The finding of the monsoon mean state regulation provides an important insight into IOD dynamics. It has potential applications in diagnosing the deficiencies of IOD simulations in the current coupled models [*Saji et al.*, 2006; L. Liu et al., Dynamic and thermodynamic air-sea coupling associated with the Indian Ocean Dipole diagnosed from 23 WCRP CMIP3 models, submitted to Journal of Climate, 2010], and in identifying the future projection of the IOD under global warming. Recall that both the mean monsoon convection and the background vertical shear are crucial in reproducing realistic precipitation and wind anomalies. Thus a failure in simulating the mean state may inhibit the ability of coupled models in reproducing realistic IOD events in the present and future climate.

[22] **Acknowledgments.** We wish to thank two anonymous reviewers for their useful comments. This work was supported by Chinese MoST grants 2006CB403602, 2009DFA21000, 2010CB950303. Tim Li was supported by ONR grant N000141010774 and First Institute of Oceanography, State Oceanic Administration, China, and by the International Pacific Research Center that is sponsored by the JAMSTEC, NASA (NNX07AG53G) and NOAA (NA09OAR4320075). This is SOEST contribution 8063 and IPRC contribution 742.

References

Adler, R. F., et al. (2003), The Version-2 Global Precipitation Climatology Project (GPCP) monthly precipitation analysis (1979–present), *J. Hydrometeorol.*, *4*, 1147–1167, doi:10.1175/1525-7541(2003)004<1147:TVGPCP>2.0.CO;2.

Bjerknes, J. (1969), Atmospheric teleconnections from the equatorial Pacific, *Mon. Weather Rev.*, *97*, 163–172, doi:10.1175/1520-0493(1969)097<0163:ATFTEP>2.3.CO;2.

Gill, A. E. (1980), Some simple solutions for heat-induced tropical circulation, *Q. J. R. Meteorol. Soc.*, *106*, 447–462, doi:10.1002/qj.49710644905.

Guilyardi, E., P. Braconnot, F.-F. Jin, S. T. Kim, M. Kolasinski, T. Li, and I. Musat (2009), Atmosphere feedbacks during the ENSO in a coupled GCM with a modified atmospheric convection scheme, *J. Clim.*, *22*, 5698–5718, doi:10.1175/2009JCLI2815.1.

Halkides, D. J., and T. Lee (2009), Mechanisms controlling seasonal-to-interannual mixed layer temperature variability in the southeastern tropical Indian Ocean, *J. Geophys. Res.*, *114*, C02012, doi:10.1029/2008JC004949.

Halkides, D. J., W. Han, and P. J. Webster (2006), Effects of the seasonal cycle on the development and termination of the Indian Ocean Zonal Dipole Mode, *J. Geophys. Res.*, *111*, C12017, doi:10.1029/2005JC003247.

Hong, C.-C., and T. Li (2010), Independence of SST skewness from thermocline feedback in the eastern equatorial Indian Ocean, *Geophys. Res. Lett.*, *37*, L11702, doi:10.1029/2010GL043380.

Hong, C.-C., T. Li, and J.-S. Kug (2008a), Asymmetry of the Indian Ocean Dipole. Part I: Observational Analysis, *J. Clim.*, *21*, 4834–4848, doi:10.1175/2008JCLI2222.1.

Hong, C.-C., T. Li, and J.-J. Luo (2008b), Asymmetry of the Indian Ocean Dipole. Part II: Model diagnosis, *J. Clim.*, *21*, 4849–4858, doi:10.1175/2008JCLI2223.1.

Jiang, X., and T. Li (2005), Re-initiation of the boreal summer intraseasonal oscillation in the tropical Indian Ocean, *J. Clim.*, *18*, 3777–3795, doi:10.1175/JCLI3516.1.

Kalnay, E., et al. (1996), The NCEP/NCAR 40-year reanalysis project, *Bull. Am. Meteorol. Soc.*, *77*, 437–471, doi:10.1175/1520-0477(1996)077<0437:TNYRP>2.0.CO;2.

Kanamitsu, M., et al. (2002), NCEP-DOE AMIP-II reanalysis (R-2), *Bull. Am. Meteorol. Soc.*, *83*, 1631–1643, doi:10.1175/BAMS-83-11-1631(2002)083<1631:NAR>2.3.CO;2.

Li, T. (1997), Air-sea interactions of relevance to the ITCZ: The analysis of coupled instabilities and experiments in a hybrid coupled GCM, *J. Atmos. Sci.*, *54*, 134–147, doi:10.1175/1520-0469(1997)054<0134:ASIORT>2.0.CO;2.

Li, T. (2006), Origin of the summertime synoptic-scale wave train in the western North Pacific, *J. Atmos. Sci.*, *63*, 1093–1102, doi:10.1175/JAS3676.1.

Li, T., B. Wang, C.-P. Chang, and Y. Zhang (2003), A theory for the Indian Ocean Dipole Zonal Mode, *J. Atmos. Sci.*, *60*, 2119–2135, doi:10.1175/1520-0469(2003)060<2119:ATFTIO>2.0.CO;2.

Roeckner, E., et al. (1996), The atmospheric general circulation model ECHAM-4: Model description and simulation of present-day climate, *Rep. 218*, 90 pp., Max-Planck-Inst. for Meteorol., Hamburg, Germany.

Saji, N. H., B. N. Goswami, P. N. Vinayachandran, and T. Yamagata (1999), A dipole mode in the tropical Indian Ocean, *Nature*, *401*, 360–363, doi:10.1038/43854.

Saji, N. H., S. P. Xie, and T. Yamagata (2006), Tropical Indian Ocean variability in the IPCC twentieth-century climate simulations, *J. Clim.*, *19*, 4397–4417, doi:10.1175/JCLI3847.1.

Smith, T. M., and R. W. Reynolds (2003), Extended reconstruction of global sea surface temperature based on COADS data (1854–1997), *J. Clim.*, *16*, 1495–1510.

Wang, B., and X. Xie (1996), Low-frequency equatorial waves in vertically sheared zonal flow. Part I: Stable waves, *J. Atmos. Sci.*, *53*(3), 449–467, doi:10.1175/1520-0469(1996)053<0449:LFEWIV>2.0.CO;2.

Wang, B., R. Wu, and T. Li (2003), Atmosphere-warm ocean interaction and its impact on Asian-Australian monsoon variation, *J. Clim.*, *16*, 1195–1211, doi:10.1175/1520-0442(2003)16<1195:AOIAII>2.0.CO;2.

Webster, P. J., A. Moore, J. Loschnigg, and M. Leban (1999), Coupled ocean-atmosphere dynamics in the Indian Ocean during 1997–98, *Nature*, *401*, 356–360, doi:10.1038/43848.

Xie, S.-P., H. Annamalai, F. A. Schott, and J. P. McCreary (2002), Structure and mechanisms of south Indian Ocean climate variability, *J. Clim.*, *15*, 864–878, doi:10.1175/1520-0442(2002)015<0864:SAMOSI>2.0.CO;2.

Yu, W., B. Xiang, L. Liu, and N. Liu (2005), Understanding the origins of interannual thermocline variations in the tropical Indian Ocean, *Geophys. Res. Lett.*, *32*, L24706, doi:10.1029/2005GL024327.

T. Li, B. Wang, and B. Xiang, Department of Meteorology, University of Hawaii, 2525 Correa Rd., Honolulu, HI 96822, USA. (timli@hawaii.edu)

W. Yu, Research Center of Ocean Climate, First Institute of Oceanography, SOA, 6 Xianxialing Rd., Qingdao 266061, China.